DISENTANGLING Mg-SUITE PETROGENESIS VIA PETROLOGICALLY HETEROGENOUS OLIVINE-HOSTED MELT INCLUSIONS IN APOLLO TROCTOLITE 76535. A. C. Stadermann[1], F. M. McCubbin[1], S. A. Eckley[2], E. W. O'Neal[2], R. S. Jakubek[2], T. M. Erickson[2], J. S. Gorce[2], K. Iacovino[2], T. C. Prissel[3], and A. Madera[1], [1]Astromaterials Research and Exploration Science, NASA Johnson Space Center (amanda.c.stadermann@nasa.gov), [2]Amentum, Astromaterials Research and Exploration Science, NASA Johnson Space Center, [3]Department of Earth, Atmospheric, and Planetary Sciences, Purdue University.

Introduction: The magnesian (Mg-) suite is a group of lithologies associated with the lunar highlands that generally consist of Mg-rich mafic phases (olivine, pyroxene) and calcic plagioclase [1]. Generally inferred to be magmatic in origin, the Mg-suite represents the earliest stage of secondary crust building on the Moon, although diverse petrogenetic models [e.g., 2–4] have been developed to understand seemingly contradictory characteristics of these rocks [5]. A key aspect of many of these models is the composition of KREEP (potassium, rare earth elements, phosphorus) incorporated into these magmas, as well as the timing and mechanism of its incorporation. Determining these factors will help discriminate between the various petrogenetic models.

Apollo 17 troctolite 76535 is a hallmark of the lunar Mg-suite, due to its relatively large mass [6], inferred pristinity [7], and ancient age [e.g., 8–10]. Olivine-hosted melt inclusions (MIs) within 76535 have been documented by previous researchers but not studied in detail [11–13]. Melt inclusions in igneous rocks are valuable because they represent pockets of melt trapped during crystallization and can provide information on magma composition and history [14, 15].

In order to better understand the role of KREEP in Mg-suite magmas and their relevance to Mg-suite petrogenesis, we are conducting a systematic study of olivine-hosted MIs in 76535, including their occurrence, size, petrology, geochemistry, and mineralogy. This work investigates 76535,218, a collection of 192 loose olivine grains that were selected based on optical identification of potential inclusions.

Methods: We have conducted a highly coordinated approach to characterizing a select subset of olivine grains petrologically, geochemically, and mineralogically. Following optical identification of potential inclusions in olivine, each grain was scanned using X-ray computed tomography (XCT) to verify internal structure, including the location and size of inclusions in the grains. Eight olivine grains were selected for further petrologic and geochemical analysis. These grains (76535,218-47, -54, -66, -133, -138, -144, -160, -174) were prepared for in situ microbeam analysis using anhydrous or dry sample preparation techniques, effectively resulting in single-crystal potted butts with inclusions of interest exposed at the surface. We characterized these grains using Raman spectroscopy, electron probe microanalysis (EPMA), energy dispersive X-ray spectroscopy (EDS), electron backscatter diffraction (EBSD), and cathodoluminescence (CL), as well as optical (transmitted and reflected) light and backscattered electron (BSE) images using instrumentation at NASA Johnson Space Center's Astromaterials Research and Exploration Science (ARES) division.

Results: The eight grains prepared in this study reveal significant MI heterogeneities, in terms of size, major phases, and internal structure in the 2D slices that we investigated. Below, we describe our characterization of these eight grains, with dimensions representing areas exposed on the polished surface. All MIs described here are mostly or entirely enclosed within their host olivine. In instances where MIs are not entirely enclosed, the overall shape of the MI in XCT was considered to be sufficiently indicative of MI origin, over any other type of trapped melt (e.g., melt embayment or late stage mesostasis).

76535,218-47 is approximately 1230×730 μm and contains two large MIs (47a and 47c) exposed on the surface. Inclusion 47a is approximately 220×100 μm and consists of an interior rich in silica (potentially tridymite), surrounded by pyroxene, with minor merrillite. Inclusion 47c is 550 μm in longest dimension and dominated by (clino- and ortho-) pyroxene, but also contains silica, merrillite, apatite, and feldspar. In addition to 47a and 47c, which were identified by XCT, the polished surface also exposes a small, <20 μm MI, denoted 47e, composed of pyroxene and feldspar.

76535,218-54 is 1090×1030 μm, with a large, 550×390 μm MI denoted 54a. Inclusion 54a contains ortho- and clinopyroxene, feldspar, tridymite, Fe-Ni metal, and a 40×25 μm baddeleyite surrounded by a thin rim of zircon. In addition to 54a, a small <20 μm inclusion 54b was identified, consisting of pyroxene, feldspar, and metal.

76535,218-66 is 1330×760 μm in size with a 150×130 μm MI, 66b (Figure 1a). This MI consists of predominantly orthopyroxene, with minor/trace clinopyroxene, K-feldspar, chromite, metal, and baddeleyite. Quantitative P maps from EPMA showed that the surrounding olivine is depleted in P approximately 40–90 μm from the exterior rim of 66b.

76535,218-133 is 1000×750 μm and contains MI 133a, ~200×230 μm (Figure 1b). Inclusion 133a has an interior rich in tridymite and K-feldspar, surrounded by clino- and orthopyroxene. Minor and trace phases

include Fe-Ni metal, baddeleyite, merrillite, chromite, troilite, and pyrochlore.

76535,218-138 is 1350×890 μm, containing MI 138a, approximately 340×240 μm. This grain includes a chromite vein roughly perpendicular to the polished surface and does not intersect inclusion 138a. Inclusion 138a is predominantly orthopyroxene, but also contains baddeleyite, merrillite, chromite and metal.

76535,218-144 is 1680×1240 μm and contains MI 144a. This grain also includes a symplectite assemblage below the polished surface of the grain. Inclusion 144a is 340×200 μm and consists of orthopyroxene, K-feldspar, and chromite.

76535,218-160 is 750×590 μm and contains two inclusions of similar size. Only inclusion 160a is exposed on the surface, approximately 80×45 μm. Inclusion 160a contains clino- and orthopyroxene, merrillite, feldspar, and metal/troilite.

76535,218-174 is 1490×1000 μm in size, containing chromite veins along fractures. Inclusion 174a is 300×210 μm in size, containing ortho- and clinopyroxene, K-feldspar, Fe-Ni metal, chromite, merrillite, quartz, zircon, baddeleyite, troilite, and loveringite (Figure 1c). Small (<30 μm) symplectites appear along the outer edge of MI 174a, consisting of chromite, clino- and orthopyroxene, similar to symplectites observed in other symplectites observed in 76535 [e.g., 12]. The baddeleyite exhibits tetragonal phase heritage, but the zircon and merrillite do not produce EBSD diffraction patterns, indicating they do not have long-range order. Some Fe-Ni metal grains in 174a contain significant amounts of Cl, likely as lawrencite ($[Fe,Ni]Cl_2$).

Discussion & Conclusions: Our detailed characterization of these MIs reveals immense variability in size, structure, petrology, mineralogy, and geochemistry. These differences likely hold clues to understanding the crystallization of 76535 olivine, and the entrapment of the MIs. More broadly, these MIs reveal changes in magma chemistry, crystallization conditions, and potentially post-crystallization alteration of 76535. Data collection is ongoing, but we are in active development of a classification scheme for the MIs in this study, to put them within a potential petrogenetic context with each other and with other studies of 76535.

The presence of lawrencite in metal grains within MI 174a is notable. Lawrencite rapidly oxidizes and hydrates upon exposure to the terrestrial atmosphere but may hold valuable information regarding the sources of volatile elements in lunar rocks [16], particularly the association of Cl and KREEP [13, 17]. All grains included in this study have been previously allocated to researchers, and therefore were exposed to the terrestrial atmosphere prior to their allocation for our study. Our identification of this rare and scientifically significant phase highlights that highly reactive phases like lawrencite may be well-preserved in the interior portions of returned (i.e., previously allocated and no longer pristine) Apollo samples.

Acknowledgments: We thank NASA for the loan of the Apollo samples used in this study. ACS acknowledges support from a NASA Postdoctoral Program (NPP) fellowship, administered by Oak Ridge Associated Universities.

References: [1] Shearer C. K. et al. (2015) *Am. Min.* 100:1. [2] Longhi J. et al. (2010) *GCA* 74:784–798. [3] Elardo S. M. et al. (2011) *GCA* 75:3024–3045. [4] Prissel T. C. and Gross J. (2020) *EPSL* 551:116531. [5] Shearer C. et al. (2023) *RiMG* 89:147–206. [6] Gooley R. et al. (1974) *GCA* 38:1329–1339. [7] Warren P. H. (1993) *Am. Min.* 78:360–376. [8] Bogard D. D. et al. (1975) *EPSL* 26:69–80. [9] Premo W. R. and Tatsumoto M. (1992) *LPS XXII*, 381-397. [10] Borg L. E. et al. (2017) *GCA* 201:377-391 [11] Dymek R. F. et al. (1975) *LPS VI*, p. 301–341. [12] Elardo S. M. et al. (2012) *GCA* 87:154–177. [13] McCubbin F. M. and Barnes J. J. (2020) *Am. Min.* 105:1270–1274. [14] Roedder E. (1979) *Bull. de Min.* 102:487–510. [15]. Wallace P. J. et al. (2021) *Ann. Rev. EPS* 49:465–494. [16] Shearer C. K. et al. (2014) *GCA* 139:411–433. [17] Barnes J. J. et al. (2016) *EPSL* 447:84–94.

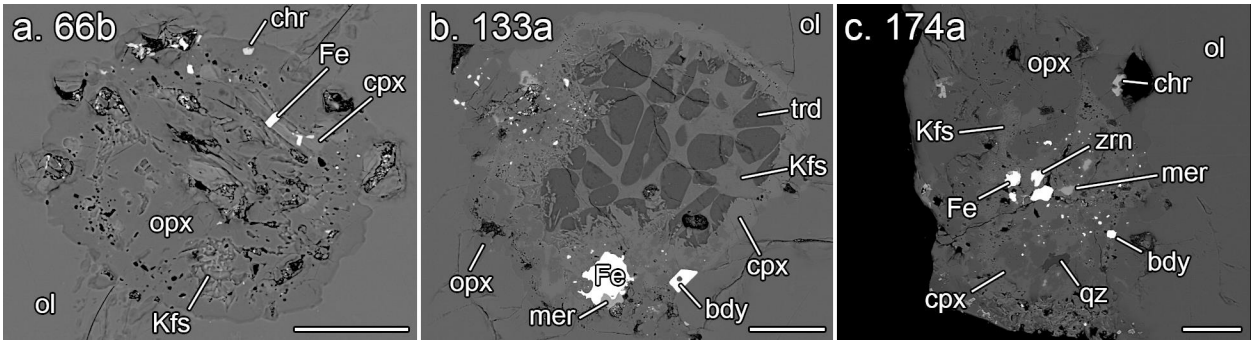

Figure 1. Backscattered electron (BSE) images of 76535 olivine-hosted melt inclusions (a) 66b, (b) 133a, and (c) 174a. All scale bars are 50 μm. Abbreviations: ol: olivine; opx: orthopyroxene; cpx: clinopyroxene; chr: chromite; Kfs: K-feldspar; Fe: Fe-Ni metal; trd: tridymite; mer: merrillite; bdy: baddeleyite; zrn: zircon; qz: quartz.